INORGANIC CHEMISTRY
FRONTIERS

RESEARCH ARTICLE

View Article Online
View Journal

Cite this: DOI: 10.1039/c6qi00584e

Dynamic structural flexibility of Fe-MOF-5 evidenced by ^{57}Fe Mössbauer spectroscopy†‡

C. K. Brozek,[a] A. Ozarowski,[b] S. A. Stoian*[b] and M. Dincă*[a]

Received 15th December 2016,
Accepted 10th January 2017

DOI: 10.1039/c6qi00584e

rsc.li/frontiers-inorganic

Temperature-dependent ^{57}Fe Mössbauer spectra were collected on Fe_xZn_{4-x}(1,4-benzenedicarboxylate)$_3$ (Fe-MOF-5). When measured under an Ar atmosphere, the data at higher temperatures reveal thermal population of the lowest-lying electronic excited state, as expected for low symmetry tetrahedral ferrous ions. In the presence of N_2, however, the temperature dependence becomes exaggerated and the spectra cannot be fitted to a single species. A fluctuating electric field gradient at the Fe nuclei best explains these data and suggests dynamic structural distortions induced by weak interactions with N_2. This direct evidence of dynamic behaviour at MOF open metal sites is relevant for the use of MOF SBUs in catalysis, gas separation, and other applications that invoke similar phenomena.

Introduction

The use of metal–organic frameworks (MOFs) for heterogeneous catalysis,[1,2] gas storage[3] and separation,[4] and detection of small molecules[5] often relies on dynamic binding of substrates to open metal sites.[6] Tuning the MOF properties for such applications is achieved by altering the composition of the molecular subunits and studying the resulting metal–substrate interactions with site-isolated precision. These interactions are intriguing because they can involve unconventional, albeit weak, bonding, such as between saturated hydrocarbons and high-spin metal centers,[4] and often require geometrical transformations to metal ion coordination spheres while maintaining structural integrity. Evidence for unconventional bonding and distortions to MOF metal sites typically lacks insight into the dynamic nature of the interactions, however. Here, we present temperature-dependent ^{57}Fe Mössbauer spectra as evidence of dynamic structural distortions at Fe sites in Fe_xZn_{4-x}(1,4-benzenedicarboxylate)$_3$ caused by weak interactions with N_2.

A family of materials known as M-MOF-5 has been useful in studying fundamental aspects of interactions between small molecules and open metal sites of MOFs. Synthesized by cation exchange of the original all-zinc MOF-5 (Zn_4O(1,4-benzenedicarboxylate)$_3$) with first row transition metal ions, M-MOF-5 preserve the crystal morphology and metal site coordination sphere of the iconic parent material, allowing the study of heterogeneous reactivity with molecular specificity.[7,8] With Ni-MOF-5, for instance, we demonstrated that MOF clusters can support unusual metal species that could undergo geometrical transformations and that these species were identifiable by spectroscopy and other physical methods. Reactivity studies of Cr- and Fe-MOF-5 proved that the metal centers could promote redox transformations of small molecules without compromising the MOF lattice. Based on the analysis of time-averaged Mössbauer spectra, we propose that the inserted Fe^{2+} centres, shown in Fig. 1, interact dynamically with N_2, leading to rapid fluctuations in the coordination environment of the Fe sites.

Results

Synthesis of Fe-doped MOF-5

Soaking the crystals of MOF-5 in a DMF solution of $Fe(BF_4)_2{\cdot}6H_2O$ for one week at room temperature furnished cubic yellow crystals of Fe-MOF-5. As discussed in previous reports,[8,9]

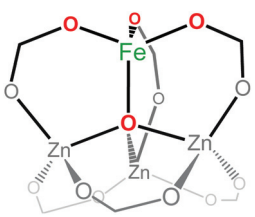

Fig. 1 Depiction of the $FeZn_3O$ cluster featured in Fe-MOF-5.

[a]*Department of Chemistry, Massachusetts Institute of Technology, 77 Massachusetts Avenue, Cambridge, Massachusetts 02139, USA. E-mail: mdinca@mit.edu*
[b]*National High Magnetic Field Laboratory, Florida State University, Tallahassee, Florida 32310, USA*

†In honor of Professor Mercouri G. Kanatzidis.

‡Electronic supplementary information (ESI) available. See DOI: 10.1039/c6qi00584e

Fe-MOF-5 crystals exhibit powder X-ray diffraction patterns, an N_2 adsorption isotherm, and a Brunauer–Emmett–Teller (BET) surface area consistent with MOF-5,[10] and Fe centers with an S = 2 ground state confirmed by SQUID magnetometry.

^{57}Fe Mössbauer spectra of N_2(l)-soaked Fe-MOF-5

To further probe the electronic structure of the Fe sites in Fe-MOF-5, we used ^{57}Fe Mössbauer spectroscopy.

After carefully optimizing the sample amount that maximized the signal-to-noise ratio, we acquired zero-field Mössbauer spectra for a non-evacuated sample at temperatures between 4.2 K and 100 K (Fig. 2). Prior to recording these spectra, the neat Fe-MOF-5 sample was stored and mounted in the spectrometer at 77 K by keeping and handling it under liquid N_2. Assuming that liquid N_2 penetrates the pores of Fe-MOF-5, we consider the sample saturated with N_2 under these conditions. At 4.2 K we observe a well-defined quadrupole doublet characterized by an isomer shift δ = 1.156(3) mm s^{-1}, a quadrupole splitting ΔE_Q = 3.02(2) mm s^{-1}, and a linewidth Γ = 0.26(1) mm s^{-1}. These values are typical of high-spin Fe^{2+} sites that have a quasi-tetrahedral coordination environment. Moreover, the rather narrow linewidth of these resonances demonstrates that at 4.2 K the coordination environment of all iron sites is nearly homogeneous. Interestingly, increasing the temperature leads to both an overall drop in the intensity of the spectra and a dramatic line broadening that is concomitant with a decrease in the apparent value of the quadrupole splitting. Thus, at 100 K the apparent quadrupole splitting contracts to ΔE_Q = 1.0(1) mm s^{-1} and the linewidth exhibits a dramatic increase to Γ = 0.80(6) mm s^{-1}. In contrast, the value of the isomer shift at 100 K remains essentially unchanged from that observed at 4.2 K. A close examination of the spectra reveals that above 4.2 K some of these resonances also exhibit a fine structure, which suggests that a differentiation in the coordination environment of the iron ions occurs with increasing temperature. The solid grey lines overlaid over the experimental data in Fig. 2 are simulations which were obtained by using the model of multidimensional hyperfine parameter distributions developed by Rancourt *et al.*[11] For this model, the distribution of a hyperfine splitting parameter, in this instance ΔE_Q, is described using a sum of individual Gaussian components. Thus, this highly unusual temperature-dependent behaviour could be rationalized only by considering three distinct components centred at ΔE_Q = 2.8(2) mm s^{-1}, 1.9(1) mm s^{-1}, and 1.2(2) mm s^{-1} (see Table S1‡). The subspectra generated by each individual component are shown as blue, pink, and red traces overlaid over the experimental data of Fig. 2. The temperature dependence of the overall distribution in the ΔE_Q value is shown in Fig. 3.

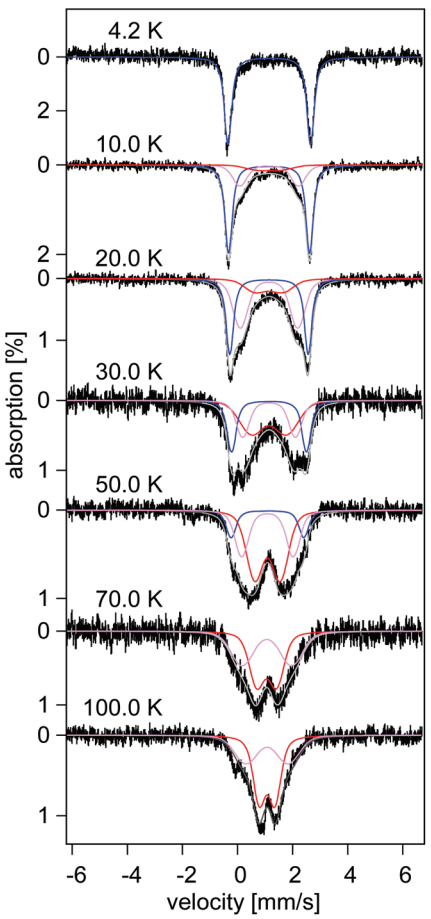

Fig. 2 Temperature dependent zero-field Mössbauer spectra recorded for a non-evacuated, N_2-soaked Fe-MOF-5 sample. The solid grey lines are simulations obtained considering a distribution in ΔE_Q values. The blue, pink and red traces illustrate the three Gaussian components of the ΔE_Q distribution.

^{57}Fe Mössbauer spectra of Fe-MOF-5 exposed to O_2(g)

To eliminate the possibility that the observed behaviour of Fe-MOF-5 was caused by O_2 contamination in the liquid N_2, we collected a Mössbauer spectrum of Fe-MOF-5 deliberately exposed to O_2. Thus, fresh Fe-MOF-5 was heated to 180 °C at 10^{-5} Torr for 24 h, then exposed to 1 atm of O_2 and sealed for 6 h. After being placed under vacuum, it was prepared for Mössbauer spectroscopy in a manner identical to the previous Fe-MOF-5 sample. As shown in Fig. S2,‡ the zero-field spec-

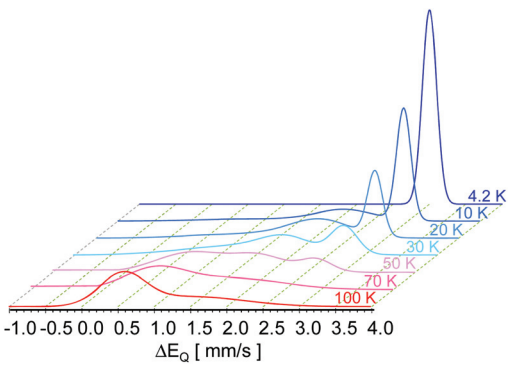

Fig. 3 Temperature dependence of the quadrupole splitting distribution observed for the zero-field Mössbauer spectra of the N_2-soaked Fe-MOF-5 sample. All curves are normalized by area.

trum of O_2-exposed Fe-MOF-5 consists of two nested quadrupole doublets at 4.2 K. Whereas the outer doublet is essentially identical to that of the starting material, the inner doublet is characterized by δ = 0.55 mm s^{-1} and ΔE_Q = 0.81 mm s^{-1}, values that are typical of high-spin ferric ions. Therefore, exposure to O_2 cannot account for the anomalous temperature dependence of the Mössbauer spectra observed in pristine Fe^{2+}-MOF-5 samples that were kept rigorously air-free.

^{57}Fe Mössbauer spectra of Fe-MOF-5 in the absence of N_2

To assess the effect of adsorbed guest molecules on the iron sites in Fe-MOF-5, we aimed to evacuate the N_2-filled sample that displayed anomalous temperature and repeat the Mössbauer experiments as before. Thus, the sample used for collecting the spectra under N_2 was placed under high vacuum for approximately 24 h, brought into an Ar-filled glovebox, and then dispersed in Paratone® N oil, which effectively seals the Fe-MOF-5 sample and prevents it from adsorbing N_2. Temperature-dependent spectra for this evacuated sample are shown in Fig. 4. The zero-field spectrum recorded at 4.2 K is characterized by an isomer shift δ = 1.149(4) mm s^{-1}, a quadrupole splitting ΔE_Q = 2.83(2) mm s^{-1}, and a linewidth Γ = 0.28(1) mm s^{-1}. These values are very similar to those observed for the N_2(l)-soaked sample. Most notably, the temperature dependence deviates greatly from that observed for the

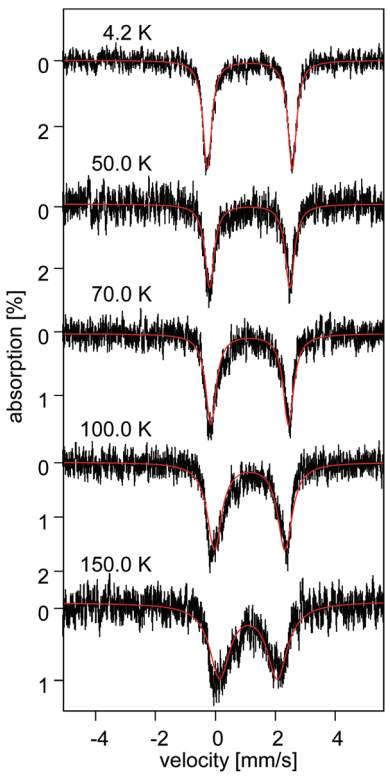

Fig. 4 Temperature dependence of the zero-field Mössbauer spectra recorded for the evacuated Fe-MOF-5 sample. The solid red lines are simulations obtained using a single quadrupole doublet. The temperature dependence of the quadrupole splitting is shown in Fig. 5.

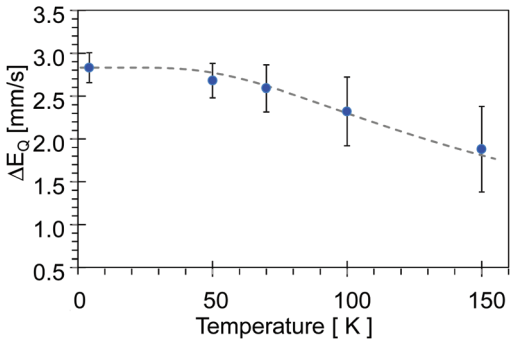

Fig. 5 The temperature dependence of the ΔE_Q (blue circles) determined for the evacuated Fe-MOF-5 sample. The length of the error bars is set equal to the observed linewidths. The dotted line is a theoretical trace obtained for an energy of the lowest excited orbital state Δ = 160 cm^{-1}, see text.

N_2(l)-soaked sample. Although the observed isomer shift remains essentially constant, ΔE_Q decreases with increasing temperature. The apparent linewidths of the observed quadrupole doublets also increase such that at 150 K the FWHM of the individual resonances becomes nearly 1 mm s^{-1}. The linewidth increase notwithstanding, the effect is much less pronounced than that observed for the N_2-soaked Fe-MOF-5 sample and the spectra can be well described using a single spectral component, *i.e.*, a single type of iron(II) site. The stark spectral differences for N_2-filled and evacuated Fe^{2+}-MOF-5 are further illustrated in Fig. S3,‡ which shows a side-by-side comparison of the spectra recorded at 4.2 K and 70 K.

The temperature dependence of the quadrupole splitting observed for evacuated Fe^{2+}-MOF-5 is shown in Fig. 5. For quasi-tetrahedral iron(II) sites the experimental ΔE_Q temperature dependence can be related to the energy of the lowest excited electronic state. Thus, for tetrahedral sites (T_d point-group symmetry) the two lowest orbitals of a high-spin, d^6 Fe^{2+} ion are degenerate and lead to degenerate orbital states for which either a $x^2 - y^2$ or a z^2 is a doubly occupied orbital. These states are characterized by electric field gradient (EFG) tensors that have components of equal magnitude but opposite signs. In a first approximation, a lowering of the iron site symmetry leads to a splitting of these states by an energy Δ. If Δ is on the order of k_BT, increasing the temperature leads to a sizable increase in the Boltzmann population of the lowest-lying excited state. In turn, the increase in the thermal population leads to a decrease in the magnitude of the individual EFG tensor components and thus, a decrease in the observed ΔE_Q value.

This effect can be modelled using the expression $\Delta E_Q(T) = \Delta E_Q(4.2\text{ K})\cdot\tanh(\Delta/2k_BT)$ (dotted line in Fig. 5), which for the evacuated Fe-doped MOF-5 sample leads to an energy splitting of ~160 cm^{-1}.

Discussion

The temperature-dependent spectral behaviour observed for the N_2-soaked Fe-MOF-5 samples is unusual. Because the

$T > 4.2$ K Mössbauer spectra recorded for N_2-filled and evacuated samples are dramatically different, the atypical temperature dependence observed for the former clearly originates from the interaction of dinitrogen with the Fe sites in Fe-MOF-5. These interactions might lead to both static and dynamic effects. In particular, inclusion of N_2 within MOF-5 could involve the participation of one or more dinitrogen molecules in the coordination sphere of the quasi-tetrahedral Fe^{2+} ions. In turn, these weak bonding interactions can induce static or fluctuating modulation of the EFG at the Fe^{2+} sites.

The effects of fluctuating electric and magnetic fields on the Mössbauer spectra of iron sites engaged in dynamic processes were first discussed by Tjon and Blume, who put forth a theoretical model that relied on time-dependent Hamiltonians to account for Jahn–Teller distortions and vacancy hopping.[12,13] These processes yield a ground-state EFG tensor for which the largest component jumps randomly in the x, y, and z directions. Similar to our observations, low-temperature spectra analysed using this model often displayed well-defined quadrupole doublets which diminished in intensity and exhibited a collapsed quadrupole splitting as the temperature increased.

One of the first instances of a fluctuating EFG was reported by Lindley *et al.* for Fe-doped AgCl, which at 80 K displays a well-defined quadrupole doublet converging toward a single resonance at 458 K.[14] This transformation occurs without a concomitant, major change in the intrinsic intensities or linewidths of the observed resonances.[14] This behaviour was ascribed to a charge-balancing vacancy hopping randomly across the crystal. This process disrupts the ligand field around Fe, causing its EFG to approach zero. Interestingly, a temperature dependence of the zero-field Mössbauer spectra similar to that observed by Lindley *et al.* for Fe-doped AgCl and by us for Fe-MOF-5 was also reported for $[Fe(\eta^6\text{-}C_6H_6)(\eta^5\text{-}C_5H_5)][PnF_6]$ (Pn = P, As).[15,16] In the solid state, each organoiron cation is surrounded by eight anions that form a cubic cage. At low temperature, the iron-containing cation orients along a specific axis within the cage, a preferred orientation that leads to a non-zero EFG. However, as the sample is heated, the increase in thermal energy leads to random fluctuations in the orientation of the molecular cation. At high temperatures the thermally activated molecular motion causes the EFG to average to zero. In contrast to the redox-based, charge-transfer process underlying the EFG fluctuation of Fe-doped AgCl, the anomalous temperature dependence of ΔE_Q in the case of the organometallic compounds is due to the temperature-induced reorientation of the cation. Considering that the framework supporting the Fe ions in Fe-MOF-5 is redox inert, a charge transfer process cannot account for the anomalous temperature dependence of the EFG of our compound. However, the thermally activated motion of MOF-absorbed N_2 molecules, analogous to that observed for $[Fe(\eta^6\text{-}C_6H_6)(\eta^5\text{-}C_5H_5)]^+$ could, in principle, justify the observed behaviour of N_2-soaked Fe-MOF-5.

To evaluate this hypothesis, we investigated the interaction of N_2 molecules with Fe-MOF-5 using density functional theory (DFT) calculations. For this purpose, we used a truncated structural model where a single $FeZn_3O$ cluster was considered, with six benzoate groups replacing the terephthalates in the actual MOF (Fig. 6). The calculations employed the B3LYP/6-311G functional/basis set and monitored the predicted zero-field Mössbauer parameters for cases where up to four dinitrogen molecules are in the vicinity of the Fe atom (see Fig. S3 and Table S4‡). Geometry optimizations of structures that included one or more dinitrogen molecules revealed a preferred end-on binding mode. Furthermore, the relaxed scan of the angle formed by the N donor atom of the N_2 moiety with iron and one of the carboxylate oxygen (N–Fe–O_c) bond angles (Fig. 6) revealed the presence of two distinct energy minima. In these calculations, we fixed the value of the N–Fe–O_c bond angle and allowed all other coordinates to be optimized. In Fig. 6 the individual minima are labelled 1 and 2, respectively. An overlay of the two geometry optimized structures obtained at minima 1 and 2 is shown in Fig. 6 and the corresponding coordinates are listed in Table S4.‡ In the absence of N_2, the Fe site has an approximate C_{3v} point group symmetry. At energetic minimum 1, the N_2 moiety occupies an apical position that is collinear with the C_3 axis of the Fe site and *trans* to the μ_4-O ligand. At minimum 2, N_2 sits in the σ_v plane that bisects the O_c–Fe–O_c angle and equatorial with Fe and carboxylate O atoms. Given the three-fold symmetry of the Fe centre, three equatorial sites are therefore available to N_2,

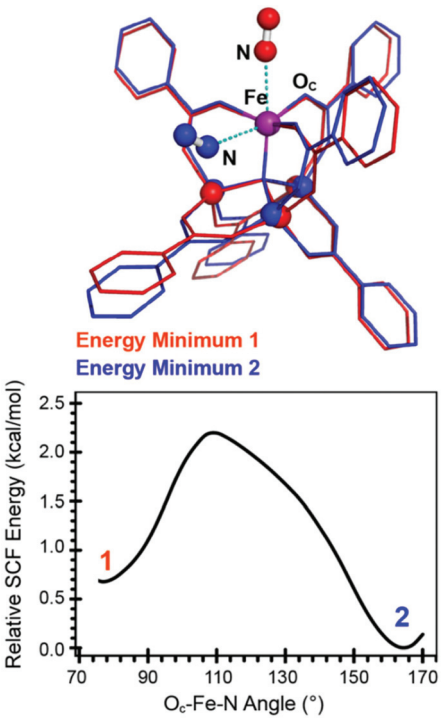

Fig. 6 Top: Overlay of the geometry optimized structures obtained at the energy minima 1 (shown in red) and 2 (shown in blue). Bottom: Relative SCF energies predicted for the relaxed scan of the N–Fe–O_c bond angle.

in addition to the apical site. Consequently, an iron site in Fe-MOF-5 can interact with up to four dinitrogen molecules. Although the predicted self-consistent field (SCF) energy for the interaction of N_2 with the Fe at an equatorial site is ~0.7 kcal mol^{-1} lower than at the apical site, the predicted Fe–N distance is considerably elongated from 2.68 Å (at apical) to 2.91 Å (at equatorial). This observation strongly suggests that N_2 interaction at an equatorial site is further stabilized by the interaction with the two adjacent Zn ions (the shortest N–Zn distances are 3.19 and 3.64 Å). Inspection of the calculated EFG tensors and zero-field Mössbauer parameters suggests that interaction of a single N_2 molecule in the apical or equatorial sites leaves the ground state EFG tensor, and thus the quadrupole splitting, essentially intact. Instead, we only observe a modest increase in the energy of the lowest energy d orbital (as predicted by TD-DFT; 14% for apical and 33% for equatorial). These observations suggest that the thermal-induced hopping of a single N_2 molecule between the two minima cannot account for the observed temperature dependent behaviour of the experimental EFG tensor. Instead, the largest changes in the ground state EFG tensor are induced by the full occupancy of the three equatorial sites, that is, three N_2 moieties interacting simultaneously with the Fe site. When compared to the N_2-free cluster, the concomitant binding of three dinitrogen molecules to equatorial sites leads to the largest modulation of the EFG tensor, in particular of the *y*-component of the EFG tensor and of the change in the ΔE_Q sign. Interestingly, full occupancy of the three equatorial sites (or equatorial and apical sites) leads to a nearly 25% decrease in energy for the average Fe–N_2 interaction. This finding suggests that the adsorption of N_2 in Fe-MOF-5 involves the transient occupation of at least three of the four sites available for interaction with N_2.

Experimental methods

Unless otherwise stated, all materials were treated as air sensitive and were manipulated using common Schlenk and inert atmosphere glovebox techniques.

Materials

Dry, deaerated dichloromethane (DCM, HPLC grade, Honeywell) and DMF (99.8%, VWR) were obtained by degassing with a flow of argon gas for 30 min and by passing the solvent through two silica columns in a Glass Contour Solvent System. 70% HNO_3 (ICP-AES grade, EMD), $Fe(BF_4)_2{\cdot}6H_2O$ (97%, Sigma-Aldrich), $Zn(NO_3)_2{\cdot}6H_2O$ (99%, Alfa Aesar), and terephthalic acid (Sigma-Aldrich) were used without further modification. MOF-5 was prepared according to the literature.[10]

Physical measurements

Powder X-ray diffraction (PXRD) patterns were recorded on a Bruker Advance II diffractometer equipped with $\theta/2\theta$ Bragg–Brentano geometry and Ni-filtered Cu-Kα radiation (Kα = 1.5406 Å). The tube voltage and current were 40 kV and 40 mA, respectively. Samples for PXRD were prepared by placing a thin layer of the sample on a zero-background silicon crystal plate supported on a cup with a dome that screwed-on with a rubber O-ring fitting.

A Micromeritics ASAP 2020 Surface Area and Porosity Analyzer was used to measure nitrogen adsorption isotherms. Oven-dried sample tubes equipped with TranSeals® (Micrometrics) were evacuated and tared. Samples were transferred to the sample tubes, heated to 200 °C for 12 h, and held at that temperature until the outgas rate was less than 2 mTorr per minute. The evacuated sample tubes were weighed again and the sample mass was determined by subtracting the mass of the previously tared tube. N_2 isotherms were measured using liquid nitrogen baths (77 K). UHP grade (99.999% purity) N_2 and He, oil-free valves and gas regulators were used for all free space corrections and measurements.

Iron and zinc analyses were conducted at the MIT Center for Materials Science and Engineering Shared Experimental Facility (CMSE-SEF) using a HORIBA Jobin ACTIVA inductively coupled plasma atomic emission spectrometer (ICP-AES). Standards were prepared from solutions purchased from ULTRA Scientific© designated suitable for ICP analysis. Elemental analysis was performed by Complete Analysis Laboratories, Parsippany, NJ.

Temperature-dependent ^{57}Fe Mössbauer spectra were recorded using a constant acceleration spectrometer. The instrument was fitted with a liquid helium cooled Janis 8DT Super Varitemp cryostat and an 8 T American Magnetics superconducting magnet. The ^{57}Co source consisted of 100 mCi ^{57}Co dispersed in a rhodium metal foil. The isomer shift values are reported against the centre of a RT spectrum recorded for a foil of α-Fe. The absorbers used during this investigation were prepared using naturally abundant iron and were enclosed in custom made polyethylene absorbers. Spectral simulations were performed using WMOSS (SeeCo, formerly Web Research Co., Edina, MN). Selected, temperature-dependent zero-field spectra were also analysed using a model of multidimensional hyperfine parameter distributions developed by Rancourt *et al.*

Synthesis of $Zn_{4-x}Fe_xO_{13}C_{24}H_{12}$ (Fe-MOF-5)

Evacuated MOF-5 crystals (490 mg, 0.636 mmol) were suspended in 40 mL of DMF and allowed to sit for one minute. A solution of 990 mg (2.93 mmol) of $Fe(BF_4)_2{\cdot}6H_2O$ in 20 mL of DMF was added to this suspension in a 100 mL jar. This material was stirred gently for a week and subsequently washed and activated in a manner typical for MOF-5 to obtain cubic yellow crystals.

Partial oxidation of Fe-MOF-5 by O_2

A dry 10 mL Schlenk flask was charged with 100 mg of yellow Fe-MOF-5 and heated to 120 °C at 10^{-5} Torr for 18 h. While maintaining heat, the flask was then backfilled with 1 atm of dry O_2 and sealed for 6 h, at which point the material appeared

bright orange. The flask was returned to vacuum, then brought into an Ar-filled glovebox to prepare as a sample for Mössbauer spectroscopy.

Computational methods

Density functional theory (DFT) calculations were performed using the quantum chemical software package Gaussian 09 C01; see ref. S2 of the ESI.‡ All calculations were performed considering a quintet ground spin state using the B3LYP/6-311G functional/basis set combination. Single point SCF calculations and geometry optimizations were completed using standard convergence criteria. For each state, ground state character of the respective electronic configuration was confirmed using time-dependent (TD)-DFT calculations which gave only positive excitation energies. The geometry optimizations of Fe-MOF-5 and (N_2)Fe-MOF-5 structures at minima 1 and 2 were followed by analytical frequency calculations, which allowed us to confirm the presence of a true minimum for each stationary structure. The EFG parameters, ΔE_Q and η were calculated using the Gaussian 09 properties, prop, keyword, and the efg option. The predicted isomer shifts were determined from the values of charge densities at the ^{57}Fe nuclei using the calibration of Vrajmasu *et al.*[17]

Optimization of the Mössbauer absorbers' thickness

The initial 80 K, zero-field spectrum of Fe-MOF-5 was recorded using a standard 8 mCi ^{57}Co source. To our surprise, even after several weeks of data collection, the signal we observed was barely larger than twice the noise level of the baseline. Consequently, to improve the statistics of our spectra we switched to a 100 mCi source. Furthermore, we optimized the effective thickness of the absorber, that is, the amount of ^{57}Fe in the path of the γ rays, to maximize the signal strength while at the same time minimizing the non-resonant absorption of the 14.4 keV radiation by the Zn ions present in a large excess. The relative strength of a Mössbauer spectrum is determined not only by the intensity of the ^{57}Co source and the amount of ^{57}Fe contained by the sample but also by the fraction of the incoming radiation that is non-resonantly absorbed. Thus, the signal-to-noise (STN) ratio is dependent on the sample thickness t', such that $\mathrm{STN}(t') \propto t' \propto e^{-t'\mu_e/2}$, where μ_e represents the total mass absorption coefficient of the sample.[18] This coefficient is an additive quantity and was calculated from the sum of the individual mass absorption coefficients of the elements present in the sample weighted by their concentration. At 14.41 keV, the absorption coefficient for Zn is 92 $cm^2\ g^{-1}$, whereas for Fe it is only 75 $cm^2\ g^{-1}$. With at least 3 Zn for every Fe in the material, most irradiated 14.41 keV light was not available for Fe to absorb.

Conclusions

^{57}Fe Mössbauer spectra of Fe-MOF-5 under Ar display a temperature dependence that becomes pronounced under an N_2 atmosphere. Mössbauer spectroscopy measurements of the latter indicate the presence of multiple Fe species. A comparison with the spectra of Fe-MOF-5 treated with O_2 rules out oxidation of the Fe sites by O_2 contaminants. Taken together, these results provide evidence that the inserted ferrous sites possess both the flexibility and reactivity to interact with N_2. Such subtle phenomena can be documented with precision, shedding light on previous reactivity studies of Fe-MOF-5 and inspiring new directions for the use of MOFs containing open metal sites for applications relying on heterogeneous reactivity.

Acknowledgements

Synthetic work in the Dincă lab was supported by a CAREER award to M. D. from the National Science Foundation (DMR-1452612). The Mössbauer spectra were recorded at the NHMFL, which is funded by the NSF through the Cooperative Agreement No. DMR-1157490, the State of Florida, and the DOE. The Mössbauer spectrometer was purchased using the NHMFL User Collaboration Grant Program (UCGP-5064) awarded to A. O. S. A. S. acknowledges partial support through the Jack E. Crow NHFML fellowship. This research was also supported in part by the NSF through TeraGrid resources provided by TACC under grant number TG-CHE150036 to S. A. S.

Notes and references

1 D. J. Xiao, E. D. Bloch, J. A. Mason, W. L. Queen, M. R. Hudson, N. Planas, J. Borycz, A. L. Dzubak, P. Verma, K. Lee, F. Bonino, V. Crocellà, J. Yano, S. Bordiga, D. G. Truhlar, L. Gagliardi, C. M. Brown and J. R. Long, *Nat. Chem.*, 2014, **6**, 590.
2 E. D. Metzger, C. K. Brozek, R. J. Comito and M. Dincă, *ACS Cent. Sci.*, 2016, **2**, 148.
3 M. Dincă, A. Dailly, Y. Liu, C. M. Brown, D. a. Neumann and J. R. Long, *J. Am. Chem. Soc.*, 2006, **128**, 16876.
4 E. D. Bloch, W. L. Queen, R. Krishna, J. M. Zadrozny, C. M. Brown and J. R. Long, *Science*, 2012, **335**, 1606.
5 M. G. Campbell, S. F. Liu, T. M. Swager and M. Dincă, *J. Am. Chem. Soc.*, 2015, **137**, 13780.
6 T. L. Easun, F. Moreau, Y. Yan, S. Yang and M. Schröder, *Chem. Soc. Rev.*, 2017, **46**, 239.
7 C. K. Brozek and M. Dincă, *Chem. Sci.*, 2012, **3**, 2110.
8 C. K. Brozek and M. Dincă, *J. Am. Chem. Soc.*, 2013, **135**, 12886.
9 C. K. Brozek, J. T. Miller, S. A. Stoian and M. Dinca, *J. Am. Chem. Soc.*, 2015, **137**, 7495.
10 S. S. Kaye, A. Dailly, O. M. Yaghi and J. R. Long, *J. Am. Chem. Soc.*, 2007, **129**, 14176.
11 D. G. Rancourt and J. Y. Ping, *Nucl. Instrum. Methods Phys. Res., Sect. B*, 1991, **58**, 85.
12 J. Tjon and M. Blume, *Phys. Rev.*, 1968, **165**, 456.
13 M. Blume and J. A. Tjon, *Phys. Rev.*, 1968, **165**, 446.

14 D. Lindley and P. Debrunner, *Phys. Rev.*, 1966, **146**, 199.
15 B. W. Fitzsimmons and A. R. Hume, *J. Chem. Soc., Dalton Trans.*, 1980, 180.
16 B. W. Fitzsimmons and W. G. Marshall, *J. Chem. Soc., Dalton Trans.*, 1992, 73.
17 V. Vrajmasu, E. Munck and E. L. Bominaar, *Inorg. Chem.*, 2003, **42**, 5974.
18 P. Gütlich, E. Bill and A. X. Trautwein, in *Mössbauer Spectroscopy and Transition Metal Chemistry*, Springer Berlin Heidelberg, Berlin, Heidelberg, 2011, pp. 541–556.